ISME

www.nature.com/ismecomms

ARTICLE OPEN

Microbial phosphorus recycling in soil by intra- and extracellular mechanisms

Jie Chen[1,2,3,4]✉, Han Xu[1], Jasmin Seven[3], Thomas Zilla[3], Michaela A. Dippold[2,5,7] and Yakov Kuzyakov[3,4,6,7]

Rising global stoichiometric imbalance between increasing nitrogen (N) availability and depleting phosphorus (P) resources increases the importance of soil microbial P recycling. The contribution of extra- versus intracellular P (re-)cycling depending on ecosystem nutrient status is vastly unclear, making soil microorganisms a blind spot in our understanding of ecosystem responses to increasing P deficiency. We quantified P incorporation into microbial DNA and phospholipids by ^{33}P labeling under contrasting conditions: low/high P soil × low/high carbon (C)NP application. By combining ^{33}P and ^{14}C labeling with tracing of microbial community biomarkers and functional genes, we disengaged the role of DNA and phospholipids in soil P cycling. Microorganisms in low P soil preferentially allocated P to phospholipids with an acceleration of phospholipids metabolism driven by C addition, which was strongly related to high abundances of microbial community members (e.g. some G-) with a fast phospholipids turnover. In high P soil, however, more P was allocated to DNA with a microbial functional shift towards DNA synthesis to support a replicative growth when sufficient C was supplied, which was coupled with a strong enrichment of fungal copiotrophs and microbial genes coding DNA primase. Consequently, adaptation to low P availability accelerated microbial intracellular P recycling through reutilization of the P stored in phospholipids. However, microorganisms under high P availability commonly adopted extracellular P recycling with release and reuse of DNA P by microbial death-growth dynamics. These results advance our understanding on microbial adaptation to P deficiency in soil by regulating component-specific P pathways and reflect the specific functions of phospholipids and DNA for P recycling.

ISME Communications; https://doi.org/10.1038/s43705-023-00340-7

INTRODUCTION

The continuously increasing N deposition in natural ecosystems are not paralleled by a similar increase in P inputs, which creates a N:P imbalance that may increase P limitation and induce significant alterations in structure and functions of natural forest ecosystems [1]. In contrast to plant adaptations, the P utilization strategies by microorganisms and their consequences for ecosystem P cycling in response to stoichiometric imbalance remain elusive [2–5].

Most of the P in forest soils is present as insoluble mineral and organic forms, as it is often adsorbed and precipitated with minerals and oxides or stored within plant litter residues and microbial necromass [6–8]. These P forms must be mineralized or solubilized by a specific group of microorganisms such as mycorrhizal and saprotrophic fungi, and phosphate-solubilizing bacteria to become bioavailable [9–11]. Microorganisms play on both sides of the fence as they effectively mineralize organic and solubilize precipitated forms of soil P, but conversely uptake and immobilize P from soil solution. Which process dominates depends on the interrelation of soil P and organic C status, reflected in distinct nutrient utilization modes. Microorganisms mobilize P from primary minerals and introduce it into the biogeochemical cycles, and so, work in the "nutrient acquisition" mode. In contrast, microorganisms immobilize soil available P in biomass and retain it in necromass after cell death, which consequently increases the conversion of unstable to relatively stable P pools. This P utilization process is characterized by the "nutrient conservation" mode. Clarifying the underlying mechanisms that drive microbial P cycling under contrasting P availability and the tradeoff between "acquisition" and "conservation modes" is essential to understand how soil microbial communities regulate soil P cycling and respond to global stoichiometric changes.

Soil microorganisms can mediate nutrient use efficiency, slow down the cellular turnover, or exploit poorly accessible nutrient resources in response to decrease in nutrient availability [12, 13]. These responses control soil nutrient cycles and, by that, plant nutrient availability. For example, microorganisms tend to adopt a recycling strategy under nutrient limitation, i.e. retain P without release and efficiently reuse it intracellularly whenever an adaptation of the molecular cell composition is needed [3, 6, 14]. Under conditions rich in both C and nutrients, however,

[1]Research Institute of Tropical Forestry, Chinese Academy of Forestry, 510520 Guangzhou, China. [2]Biogeochemistry of Agroecosystems, Department of Crop Sciences, University of Göttingen, 37077 Göttingen, Germany. [3]Soil Science of Temperate Ecosystems, University of Göttingen, 37077 Göttingen, Germany. [4]Agricultural Soil Science, Department of Crop Science, University of Göttingen, 37077 Göttingen, Germany. [5]Geo-Biosphere Interactions, Department of Geosciences, University of Tuebingen, 72076 Tuebingen, Germany. [6]Peoples Friendship University of Russia (RUDN University), 117198 Moscow, Russia. [7]These authors jointly supervised this work: Michaela A. Dippold, Yakov Kuzyakov. ✉email: chenjiecaf@hotmail.com

Received: 17 July 2023 Revised: 20 November 2023 Accepted: 22 November 2023
Published online: 24 January 2024

microorganisms are proposed to drive an acquiring strategy, i.e. immobilize and mobilize P during rapid growth and death but also exudation, providing available P for plant or microbial uptake [14–17]. Thus, P-containing components released from microbial cells are important resources for bioavailable P in ecosystems [18, 19]. In consequence, characterizing the turnover of P-containing cellular metabolites under varied nutrient conditions will provide an improved mechanistic understanding of microbial P cycling in ecosystems.

Depending on the most deficient element for microbial growth, C amendments in soils mostly convert dormant microbes to an active physiological state [15, 20]. Microbial P turnover under both dormant and active state is tightly coupled to C metabolisms. Carbon not only serves as energy resource for microbial P mobilization and uptake, formation of P compounds (e.g., DNA, RNA, phospholipids and ATP), and cell growth; but is also required for synthesizing P-containing cell components, i.e. forms the backbone of organic P metabolites [21]. Replicative microbial biomass growth after activation usually follows an exponential increment in nucleic acids, which is expressed by substantial incorporation of C and nutrients into microbial biomass [22, 23]. Nevertheless, it remains unknown whether the activation of cell metabolism up to replicative growth will alter the P distribution among cell components.

The two main cell components to which P is allocated after microbial immobilization are nucleic acids (DNA and RNA; indicative for growth by cell replication) and phospholipids of the cell membranes [3]. Together, these pools contain 80% of the total P in microbial biomass [24]. Accordingly, the regulation of P allocation into these two central cellular P pools dominates the cellular P partitioning in microbial biomass but after cell death also necromass. Fast-replicating microorganisms may invest substantial P to nucleic acids because a large amount of DNA and ribosomal RNA is required for rapid protein synthesis to support cell division and replicative growth [25]. Moreover, reparation of damaged DNA and even multiple rounds of replication DNA even occur before the formation of daughter cells, the step requiring membrane lipid formation [26]. Thus, both DNA replication and repairation require phosphate to rebuild the DNA backbones. All these promote the suggestion that activation of cell metabolism up to replicative growth probably lead to a greater nucleic acid P incorporation – a recognition underlined in the "growth rate hypothesis" [27].

Microbial community structure plays a crucial role in the distribution of cellular nutrients because various microbial groups feature specific cellular structures with defined element demands [28, 29]. In particular, G- bacteria have an additional phospholipid bilayer in the outer cell membrane as part of the cell wall, leading to higher P incorporation into phospholipids than in G+ bacteria [20, 30]. Given the greater surface-to-volume ratio and thus higher demand for cell membrane compounds such as phospholipids, bacteria typically have a higher phospholipids P content than fungi [31], making them often more sensitive to changing P availability. Besides, microorganisms can reshape the composition of their membrane lipids to acclimate to harsh environments including depleted substrate availability, freezing, low pH, and drought [32, 33], which may cause considerable variations in phospholipids P content in response to environmental changes. Warren et al. [34] recently demonstrated for P-limited Australian forest soils that microorganisms could substitute phospholipids by a P-free analog – the betaine lipids to resist to low P stress, which may lead to P depletion in membrane lipids and probably promote an intracellular P re-allocation. This raises the question whether phospholipids P can serve as a variable P storage that can be potentially depleted via intracellular recycling under strong P limitation.

This study was designed to investigate microbial P immobilization into biomass and to monitor allocation of the immobilized P between DNA and phospholipids by using ^{33}P labeling. Two temperate beech forest soils with contrasting P availability (i.e., high P and low P soils) were chosen as the model soils for the ecosystems representing a strongly acquiring and a highly recycling nutritional modes, respectively, as proposed by Lang et al. [18]. Our previous study has demonstrated contrasting pathways of microbial nutrient turnover in these soils, i.e., microbial growth and death through necromass reutilization in the high P soil and microbial maintenance through intracellular metabolisms in the low P soil [15]. These findings provide the evidences for an acquiring nutrient strategy adopted by microorganisms in the high P soil while a recycling nutrient strategy for microorganisms in the low P soil, which demonstrates that the ecosystem nutritional modes are strongly associated with microbial P nutrition strategies. However, the patterns in microbial P allocation towards various cellular P pools, their intra- versus extracellular dynamics and the potential consequences for microbial P turnover in these acquiring and recycling systems are poorly understood.

We performed an incubation study, first adding P to remove the effect of P limitation on P allocation. Three days later, we added C to test if the P allocation is influenced by C availability; any potential N limitation was avoided by co-occurring N amendment. By analyzing the incorporation of labeled P into DNA and phospholipids depending on P and C availability, and by linking the incorporation pattern to microbiome compositional and functional shifts, the intracellular P allocation strategies of soil microorganisms were traced. We hypothesize that: (i) microbial reallocation of immobilized P between the cellular pools will show strong dependence on soil P availability. Specifically, in low P soil the newly available P in soil solution will be preferentially incorporated into phospholipids to serve as a variable P storage that can be intracellularly recycled under strong P limitation, leading to a high P turnover in phospholipids (hereafter referred to as the phospholipids P incorporation pattern). In high P soil microorganisms will incorporate more P into DNA than into phospholipids, leading to a fast DNA P turnover (hereafter referred to as the DNA P incorporation pattern). This is because more P will be invested for DNA repairation or duplication than for cellular storage when the microorganisms are not nutrient limited and are ready to grow upon C provision. (ii) As soil microbiomes are generally C limited [35], both phospholipids and DNA P incorporation will be intensified under increased C availability, inducing microbial growth. (iii) Increase in C availability will intensify the contrasting P incorporation of microbiomes mainly by shifting their composition towards a stronger representation of their functional traits. We expect a boost of G- bacteria driven by increased C availability under the phospholipids P incorporation pattern. This is because a higher relative abundance of G- will result in a higher incorporation rate of P into phospholipids, as the G- require two phospholipid layer to form the cell membranes. We also expect a higher abundance of functional genes coding enzymes involved in phospholipids metabolisms and DNA biosynthesis under the phospholipids P and DNA P incorporation patterns, respectively.

MATERIALS AND METHODS

Study sites and soil sampling

Two forest sites in Germany with contrasting P availability were selected for the experiment. The low P site Unterluess is located in the Lueneburg Heath (52°50′21.77″ N, 10°16′2.37″ E) with a mean annual precipitation of 780 mm and a mean annual temperature of 8 °C. The soil type is Spodic Cambisol developed from Pleistocene sediments. The high P site is Bad Brückenau, located in the Rhön Mountains (50°21′7.26″ N, 9°55′44.53″ E) with a mean annual precipitation of 1030 mm and a mean annual temperature of 5.8 °C; the Dystric Skeletic Cambisol here developed from basalt. The total P content in the low P soil is 195 μg g^{-1}, whereas that in the high P soil is 2966 μg g^{-1} (Table S1). The dominant tree species at both

sites is European Beech (*Fagus sylvatica* L.), with an average tree age of 120 years. Bulk soil from the A horizon was collected in November 2016. Soil samples were transported immediately to the lab, sieved (2 mm), and stored at 4 °C before the experiment.

Design on incubation experiment

The soil was adjusted to 60% water holding capacity and pre-incubated for two weeks at room temperature in glass jars with screw caps placed in an incubation chamber. During the incubation, C, N and P were added at high (H) and low (L) level, resulting in two nutrient amendments for each of the two soils (low CNP and high CNP). The element amount added in high CNP treatment was 200% relative to the initial microbial biomass C (C_{mic}), N (N_{mic}) and P (P_{mic}), whereas in the low CNP treatment, only 5% of the initial C_{mic}, N_{mic} and P_{mic} were added [15]. Each treatment had four replications.

For each replication, 80 g of fresh soil were incubated for 17 days, and the reference samples were taken at day 0 before nutrient addition. We chose to incubate the soils for 17 days because microorganisms generally passed all the states (dormant, active and potential active) within two weeks after adding easily available substrates [20]. After reference sampling, 1.5 ml of the phosphate solution labeled with 111 kBq ^{33}P-KH_2PO_4 (Hartmann Analytic GmbH, Braunschweig, Germany) were added to each sample. Three days after P addition, C and N were added as glucose and $(NH_4)_2SO_4$ in 1 ml solution, and meanwhile each incubation was labeled with 12 kBq ^{14}C-glucose (Hartmann Analytics, Germany) [15]. Soil samples were collected in the morning at days 1, 3, 4, 6, 11 and 17 during the incubation and stored at -20 °C for further analyses.

Determination of microbial biomass

Microbial biomass was determined by the fumigation extraction method [36, 37]. For the analysis of C_{mic} and N_{mic}, two sets of 10 g per sample were prepared into glass bottles. One set was fumigated with chloroform for 24 h in a vacuum and then extracted with 40 ml 0.05 M K_2SO_4, whereas the other set was directly extracted with the identical solution. Total dissolved C (TC) and N (TN) concentration of the K_2SO_4 extracts from fumigated and unfumigated samples were quantified by a total organic C analyzer (Multi N/C 2100, Analytics Jena, Germany). The difference of TC or TN between the fumigated and unfumigated samples was divided by the extraction factor 0.45 or 0.54 to gain the C_{mic} or N_{mic} content, respectively [36, 37]. We chose to use these extraction factors for both the high and low P soils, because they were widely validated in many previous studies conducting in various soils [36]. However, there still exists a strong limitation for this biomass extraction method based on the fact that the extraction factors dependent on the variable proportion of (mostly) hydrophilic biomass, which can vary if the chemical composition of microbial biomass varies. For example, if addition of C leads to PHB synthesis then a larger proportion of microbial C will not be extracted, and one would need to use a different extraction factor to compensate. Thus, a specific extraction factor should be generated under each nutrient treatment per soil in future studies.

The P_{mic} was measured by combining direct fumigation and membrane techniques [38, 39]. Briefly, 1.5–3 g dry weight equivalent of the incubated soil was shaken in 30 ml deionized water either with or without 0.3 ml chloroform in a 50 ml centrifuge tube on a horizontal shaker (150–170 rev min^{-1}) for 24 h at room temperature. Anion exchange membranes with an area of 18.75 cm^2 (551642 S, VWR International, Darmstadt, Germany) were added to each tube to absorb the extracted P. The membranes were then exchanged with 45 ml 0.25 M H_2SO_4 for 3 h to release the absorbed P. The P concentration in the H_2SO_4 solution was measured by the malachite green colorimetric procedure on a plate reader (Victor^3 1420 Multilabel counter, Perkin Elmer, Turku, Finland) at 630 nm using the "Peroxidase" protocol [15, 40]. Standards obtained from KH_2PO_4 solution with a series of P concentrations were generated for calibration. Finally, the P_{mic} was represented as the difference of P content between the fumigated and unfumigated (i.e. with and without chloroform) samples, corrected with a soil-specific extraction factor [41]. For the low P soil, we simply used the Cambisol soil-specific extraction factor 0.69 from Bilyera et al. [41], because this soil was collected from the same site used by Bilyera et al. [41] (The Cambisol). For the high P soil, however, a negative extraction factor was obtained when using the equation suggested by Bilyera et al. [41]: $Kp = 0.76 - 0.007 \times$organic C content $- 0.56 \times$ total P content $+ 0.004 \times$ Clay content, mainly due to the extraordinarily high total P content (2.9 g kg^{-1}) and organic C content (197 g kg^{-1}) in our high P soil (Table S1). Thus, the traditional average extraction factor of 0.4 was used to calculate P_{mic} in the High P soil [39].

DNA extraction, sequencing of amplifications, and bioinformatic analysis

Soil DNA was extracted with the FastDNA™ SPIN Kit for Soil (MP Biomedicals, Solon, OH, USA) according to the manufacturer's protocol [15]. The DNA extracts were quantified with the Quant-iT^{TM} PicoGreen^{TM} dsDNA Assay Kit (Sigma Aldrich, Germany). In brief, 100 µl of the 200-times diluted DNA extracts were added to 96-well microplates and mixed thoroughly with 100 µl 1×PicoGreen^{TM}. Thereafter, the microplates were read on an automated fluorometric plate reader (Victor^3 1420 Multilabel counter; Perkin Elmer, Turku, Finland) after incubation for 2 min in the dark at room temperature. The DNA concentration was calibrated by 1×TE diluted standards containing various dilutions of bacteriophage lambda dsDNA.

We amplified the V4 region of the bacterial 16 S rRNA gene with the primers 515 F/806 R and the fungal ITS1 region using the primers ITS5F/ITS2R [42, 43]. The primers were attached by a barcode in order to differentiate samples. Afterwards, PCR reactions were performed in three replications in 96-well plates (Axygen, USA) on a BioRad S1000 thermal cycler (BioRad Laboratory, CA, USA), with the conditions as follows: 94 °C for 5 min; 30 cycles of 95 °C for 30 s, 52 °C for 30 s and 72 °C for 30 s; 72 °C for 10 min. The replicated amplicons were pooled for each sample and purified with a DNA Gel Extraction Kit (Axygen Biosciences, Union City, CA, USA). Sequencing was performed on the Illumina HiSeq2500 platform (PE250) by the Genepioneer Biotechnologies Company (Nanjing, China).

The sequencing results were analyzed by the Qiime software (http://qiime.org/scripts/split_libraries_fastq.html) for assignment of sample ID based on the paired-end barcode and primers [42]. After removing the barcode and primer fragments, raw sequences were generated according to the overlap region of the merged sequences, with a minimum overlap length of 10 bp and a maximum mismatch ratio of 0.2. The raw sequences quality was then controlled by removing the reads that contained ambiguous base calls, had a quality score ≤ 20, or had a sequence length longer than 150 bp. All the high-quality sequences were clustered based on 97% identity with the uparse algorithm on Usearch V8.0.1517 to generate the OTU table. The bacterial taxonomy was assigned referring to the Ribosomal Database Project (RDP) classifier (http://rdp.cme.msu.edu/), and fungal taxonomy information was identified according to the UNITE 7.1 (ITS, http://unite.ut.ee/index.php) database [44]. All samples were rarified to 29968 for bacteria and to 20211 for fungi according to the samples with the lowest sequences number prior to further analysis. We also predicted bacterial functions using PanFP [45], and annotated the functions involved in C and P transformations against the Kyoto Encyclopedia of Genes and Genomes (KEGG) database. The raw sequence data were deposited in the Sequence Read Archive (SRA) at the US National Center for Biotechnology Information (NCBI) database under the accession number of project PRJNA860331 and Biosample SAMN29840944.

Phospholipids extraction

The intact phospholipids were extracted and purified with the method according to Frostegård et al. [46], modified by Gunina et al. [47]. Briefly, 6 g of fresh soil was extracted twice by an extraction buffer including 0.15 M citric acid, methanol, and chloroform in the ratio 0.8:2:1 (v:v:v), firstly with 18 ml and secondly with 6 ml. Afterwards, the supernatant of the extracts was separated by the liquid-liquid extraction method with citrate buffer and chloroform. Six mL of chloroform and 6 ml of 0.15 M citric acid were added to the extracts to generate a two-phase solution and the sample was shaken. The lower phase was then separated and an additional liquid-liquid extraction was performed with 12 ml chloroform. Phospholipids were separated from neutral lipids and glycolipids by solid phase extraction in columns filled with activated silica gel (Silica gel Merck, particle size 0.063–0.200 mm). Briefly, 5 ml chloroform was added to elute the first fraction (neutral lipids) and 20 mL acetone was added to elute the second fraction (glycolipids), and then the intact phospholipids were eluted in 20 ml methanol by adding 5 mL for four times. The methanol phase was concentrated by rotary evaporation and stored at −20 °C for further analysis. Thereafter, the ^{33}P activity in the extract was measured, and was then used to calculate the phospholipids P formed from P in the soil solution. Instead of the total phospholipids content, the amount of phospholipids P formed can help us distinguish the P storage between the de-novo formed and old phospholipids under the stimulation of nutrient amendments.

Determination of ^{14}C and ^{33}P activities

The DNA solution (3 ml) and phospholipids extracts (3 ml) were mixed with 6 ml and 14 ml scintillation cocktail RotiszintEcoplus (Roth, Germany),

respectively, and the ^{33}P and ^{14}C activities were measured together on a scintillation counter (HIDEX 300SL, Turku, Finland). The measurement was repeated again 2 months later, aiming to disentangle the contribution of ^{33}P and ^{14}C to the activity. Given that ^{33}P has a half-life time of 25.3 days, the decline in the activity between the two measurements is solely attributable to the ^{33}P decay. A subsample of 3 ml water extracted P was mixed with 6 ml scintillation cocktail RotiszintEcoplus and read on a scintillation counter for measurement of ^{33}P activity in the soil bioavailable P pool.

Amount of DNA P and phospholipids P formed from phosphate of the soil solution

The amount of DNA P and phospholipids P formed during the incubation was calculated as the amount of P taken up from soil solution with a distinct specific ^{33}P activity with the following equations [48]:

$$DNA-P\,formed(\mu g)=\frac{Total\,^{33}P\,in\,DNA(Bq)}{Specific^{33}P\,activity\,in\,soil\,solution(Bq(\mu gP))^{-1}} \quad (1)$$

$$phospholipids-P\,formed(\mu g)=\frac{Total\,^{33}P\,in\,phospholipids(Bq)}{Specific^{33}P\,activity\,in\,soil\,solution(Bq(\mu gP))^{-1}} \quad (2)$$

This determination of DNA P formed is based on the isotope dilution analysis with an assumption that by chemical processing the specific activity (activity per unit mass) of a mixture of stable and radioactive isotopes is not changed [48]. The specific ^{33}P activity is indicated by the ^{33}P activity per unit of water-extractable P as follows.

$$\text{Specific}\,^{33}P\,activity\left(Bq(\mu gP)^{-1}\right)=\frac{^{33}P_{water\,extract}(g\,soil)^{-1}\,(Bq)}{P_{waterextract}\,(\mu g(g\,soil)^{-1})} \quad (3)$$

Although the sorption of ^{33}P to soil matrix can strongly affect the specific ^{33}P activity, the ^{33}P sorption to the soil matrix will peak very fast after several minutes of tracer addition [49]. We therefore determined the specific ^{33}P activity at the earliest 24 h after tracer addition and assumed that the inorganic P in water extract was the bioavailable P. Thereafter, we determined the ^{33}P activity of water-extractable P at each of the six sampling dates to trace changes in the specific ^{33}P activity during the course of incubation. Meanwhile, the ^{33}P activity in both DNA and phospholipids extracts was measured to calculate the DNA P and phospholipids P formed (Eq. 1 and Eq. 2).

Statistics

We examined the effects of incubation time by one-way ANOVA, and the Tukey HSD was implemented for post-hoc multiple comparisons among time points under the homogeneity of variances (Levène test). If the homogeneity of variances was not satisfied, the nonparametric Kruskal-Wallis test was used in combination with a Bonferroni correction for multiple comparison. The effects of the treatments (i.e., high and low CNP addition) were determined by independent samples *t-tests*. All above statistics were carried out using SPSS v.16.0 (SPSS Inc., Chicago, IL, USA). Statistics on the microbial community were conducted with R 4.1.0. Differences in microbial community structure were visualized in non-metric multidimensional scaling (NMDS) plots based on Bray-Curtis dissimilarity matrices at OTU level. The pairwise comparisons of microbial structure depending on incubation duration were performed using "pairwise.adonis" in the vegan package. Relative contributions of environmental factors to differences in community structure were detected using PERMANOVA with "adonis" in the vegan package. Environmental factors were also incorporated into a canonical correspondence analysis (CCA) to further examine the drivers of shifts in microbiome structure with increase in incubation duration. The collinearity of environmental factors was assessed with "varclus" in the Hmisc package, and the highly correlated (Spearman's rho$^2 \geq 0.5$) variables were excluded prior to the PERMANOVA and CCA. Structural equation modeling (SEM) with path analysis was used to test causal relationships between CNP addition, microbial biomass stoichiometry (C_{mic}: N_{mic}: P_{mic}), DNA content, composition of bacterial and fungal communities, as well as de-novo phospholipids and DNA P formed from bioavailable P in soil solution. The covariance matrix was fitted to the model via the maximum likelihood calculation using IBM SPSS-Amos 26.0 with the Chi square ($p > 0.05$) and Root Mean Square Error of Approximation (RMSEA) < 0.05. The Comparative Fit Index (CFI) was calculated to further test the goodness of model fit.

RESULTS

Microbial growth and nutrient limitations

After P input, the DNA content remained stable irrespective of soil type, but it increased markedly by 38–125% within two days following high CN input, indicating replicative microbial growth (Table S2). In the low P soil, the contents of C_{mic} and P_{mic} but not of N_{mic} increased gradually after high level P input and peaked promptly following CN addition, with few days prior to the DNA increase (Table S2). This lag-phase of incorporation of the nutrients (C and P) into the cytosol before growth start indicated C and/or P limitation, which led to an element stoichiometric shift in microbial biomass (C_{mic}: N_{mic}: P_{mic}) from 691:105:1 to 33:2:1 (Table S2).

In high P soil, the P_{mic} increased by 1.5 times within a few days when P was applied alone, and the subsequent high level CN addition simultaneously increased C_{mic} and N_{mic} by 43% and 71%, respectively (Table S2). This led to minor changes in stoichiometry (C_{mic}: N_{mic}: P_{mic}) during microbial biomass growth. However, the subsequent low level CN addition only led to 33% increase in C_{mic}, with the N_{mic} kept unchanged, reflecting a C deficiency in microbial cells in company with increase in P incorporation.

Phosphorus incorporation into de-novo formed DNA and phospholipids

After P addition, the de-novo DNA P formed from the added phosphate initially amounted to 0.28 and 2.07 μg P g^{-1} soil in the low and high P soils, respectively. This was more than 50% higher than the de-novo formed DNA P content 2 days later, indicating temporal stimulation of DNA P incorporation (Fig. 1a, b). This matched well with the higher ^{33}P proportion allocated to the DNA (1.6%–13%) than that allocated to phospholipids (0.1%–1.4%) during these first 2 days. (Fig. 2).

After low and high levels of CN inputs into the high P soil, the de-novo DNA P increased again synchronously with a de-novo formation of phospholipids P, which was strongly coupled with the marked increase of DNA (microbial growth, Table S2, Fig. 1d). In this phase, ^{33}P incorporation into DNA (0.9% to 1.2% of ^{33}P incorporation) was higher than that into phospholipids (0.5% to 0.6% of ^{33}P incorporation), and the turnover of DNA P (18 days) was faster than that of phospholipids P (100 days) (Fig. S1b, d).

In low P soil, however, when only low level CN was added, the phospholipids P increased immediately before a marked increase in DNA content (microbial growth, Table S2, Fig. 1c). This, combined with a higher incorporation rate of ^{33}P into phospholipids (24%) than into DNA (15%), demonstrated a fill-up of the phospholipids P pool prior to replicative microbial growth following C addition (Fig. 2a, c). Meanwhile, we observed a faster turnover of phospholipids P (25 days) versus DNA P (50 days) (Fig. S1a, c).

Soil microbial community composition and its controlling factors

The top bacterial and fungal classes differed between the low and high P soils (Figs. 3a–d, 4a–d), and showed different responses to nutrient additions. Generally, the bacterial composition in low P soil was much more responsive to nutrient addition than those in high P- soil (Fig. 3c, d). In the low P soil, the relative abundance of bacterial class Betaproteobacteria increased from 37% to 50% following P input, and peaked at 60% two days after the subsequent CN addition. This was accompanied first by a drop and later by an increase in the relative abundance of classes Alphaproteobacteria, Acidobacteriia, Verrucomicrobiae and AD3 (Fig. 3a, b). Notably, the Bacteriodia nearly completely disappeared from the microbial community after P addition.

Within fungal community, CN addition increased the relative abundance of class Eurotiomycetes but reduced that of

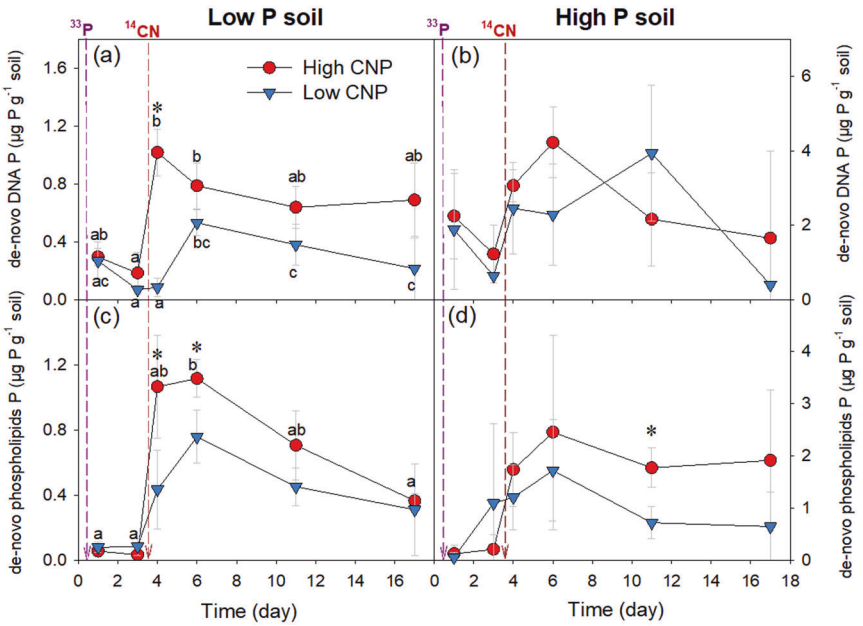

Fig. 1 Dynamics of P in de-novo DNA and phospholipids. The DNA P and phospholipids P are formed from bioavailable P taken up from the soil solution after low and high CNP addition in a low P soil (**a**, **c**) and a high P soil (**b**, **d**). Solid circles and triangles represent means, and error bars show standard deviation ($n = 4$). Purple dash arrow indicates the time of ^{33}P-phosphate addition, and red dash arrow indicates the time of ^{14}C-glucose and ammonia sulfate addition. "*" means significant difference between the two nutrient levels, and lowercase letters indicate significant difference among sampling dates within one treatment with $p < 0.05$.

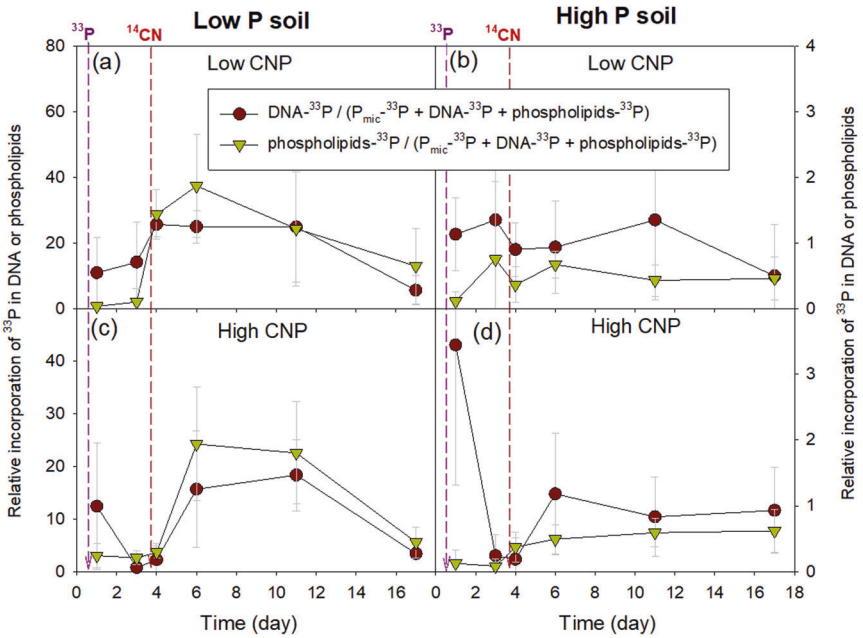

Fig. 2 Ratios of ^{33}P in DNA: ^{33}P in microbial biomass P (P_{mic}) and ^{33}P in phospholipids: ^{33}P in P_{mic}. These ratios illustrate the relative incorporation rate of P into DNA and PLFA in a low P soil (**a, c**) and a high P soil (**b, d**) amended with two levels of CNP. Purple dash arrow indicates the time of ^{33}P-phosphate addition, and red dash arrow indicates the time of ^{14}C-glucose and ammonia sulfate addition.

Mortierellomycetes in the P soil (Fig. 4a, b). In high P soil, the relative abundance of Mortierellomycetes and Agaricomycetes increased gradually from 26% and 17% under the control to 28% and 30% after P addition and further to 52% and 46% following CN application, whereas the Eurotiomycetes became less abundant after nutrient amendments (Fig. 4c, d).

About 13-59% of the microbial composition was explained by the independent and interactive effects of microbial biomass (C_{mic} and P_{mic}) and component-specific P incorporation (phospholipids P and DNA P formed) (Fig. S3e, f, S5e, f). After a single P input, the microbial shifts in low P soil were related to an increase in C_{mic} and P_{mic}, but the microbial shifts in high P soil correlated with an enrichment of de-novo formed DNA P (Figs. S3a–d, S5a–d). The microbial shifts initially induced by CN input were closely related to de-novo phospholipids P formation in both soils. The subsequent changes were strongly associated with de-novo

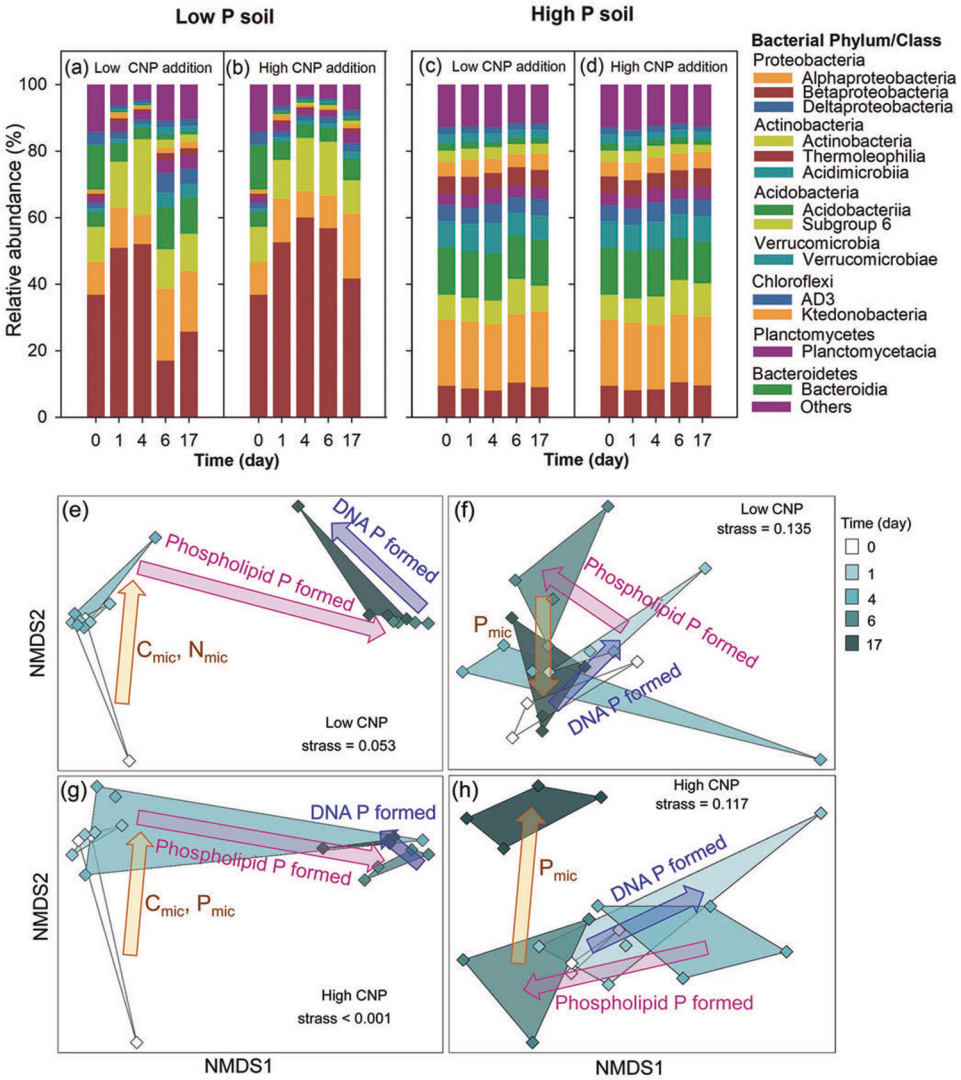

Fig. 3 Changes in relative abundance of the dominant bacterial taxa and the processes following sequential P and CN additions at two contrasting levels in the low P and high P soils. Changes in bacterial community composition are indicated by shifts in relative abundance of the top 13 bacterial classes affiliating to 7 phyla (**a**–**d**). Simplified non-metric multidimensional scaling (NMDS) plots derived from sequence data at OTU level (**e**–**h**). There are three replicates in the day 0, and four replicates in other sampling days. Areas marked by different colors in NMDS plots separate the community composition before and after CNP additions, and arrows show most important processes of microbial biomass, phospholipids P and DNA P formation (canonical correspondence analysis, $p < 0.05$).

DNA P formation in the low P soil and with P_{mic} in the high P soil (Figs. S3a–d, S5a–d).

Functional genes of C and P metabolisms

In low P soil, the relative abundance of genes involved in organic P mineralization dropped considerably following CN addition (Figs. 5a–c, S7, S8a–e). Thereafter, an increase trend in genes coding acid phosphatase (*phoN*, *olpA*) was detected (Fig. S8a–e). However, genes coding for P-transport and uptake showed an opposite pattern with the P-mining genes, i.e. they flourished after CN addition, and then gradually declined to the reference level (Fig. 5d–h, S8f–j). Overall, bacteria in the low P soil had stronger functional potential to respond to altered environmental stoichiometry than those in the high P soil, with an increased potential in P-transport and uptake while a decreased potential in P mineralization triggered by CN addition. In addition, we also found an increase in relative abundance of genes involved in carbohydrate utilization, e.g. cellulases and β-glucosidases in companying with the increased functional potentials in P -transport and uptake.

Also in low P soil, CN addition increased the relative abundance of genes responsible for microbial intracellular P metabolism, i.e. those genes catalyzing the biosynthesis or hydrolysis of glucose-6-phosphate and glycerol-3-phosphate, both of which are key precursors for phospholipids biosynthesis (Fig. 6c–i, S9e–r). In high P soil, however, genes coding putative DNA primase were enriched by CN addition (Fig. 6a, b, S9a–d).

Predictors of P incorporation into DNA and phospholipids

According to the SEM results, variations in microbial biomass, DNA content, and bacterial and fungal community compositions combined explained 25% of the changes in de-novo formed phospholipids P and 11% of the de-novo formed DNA P (Fig. S6). The bacterial composition shifts induced by CNP inputs had the strongest direct effects on the phospholipids P, followed by the direct effects of changes in C_{mic}: N_{mic}: P_{mic}. In contrast, the fungal composition shifts induced by CNP inputs had the strongest effects on the DNA P via strong direct and weak indirect impacts on DNA content (Fig. S6b).

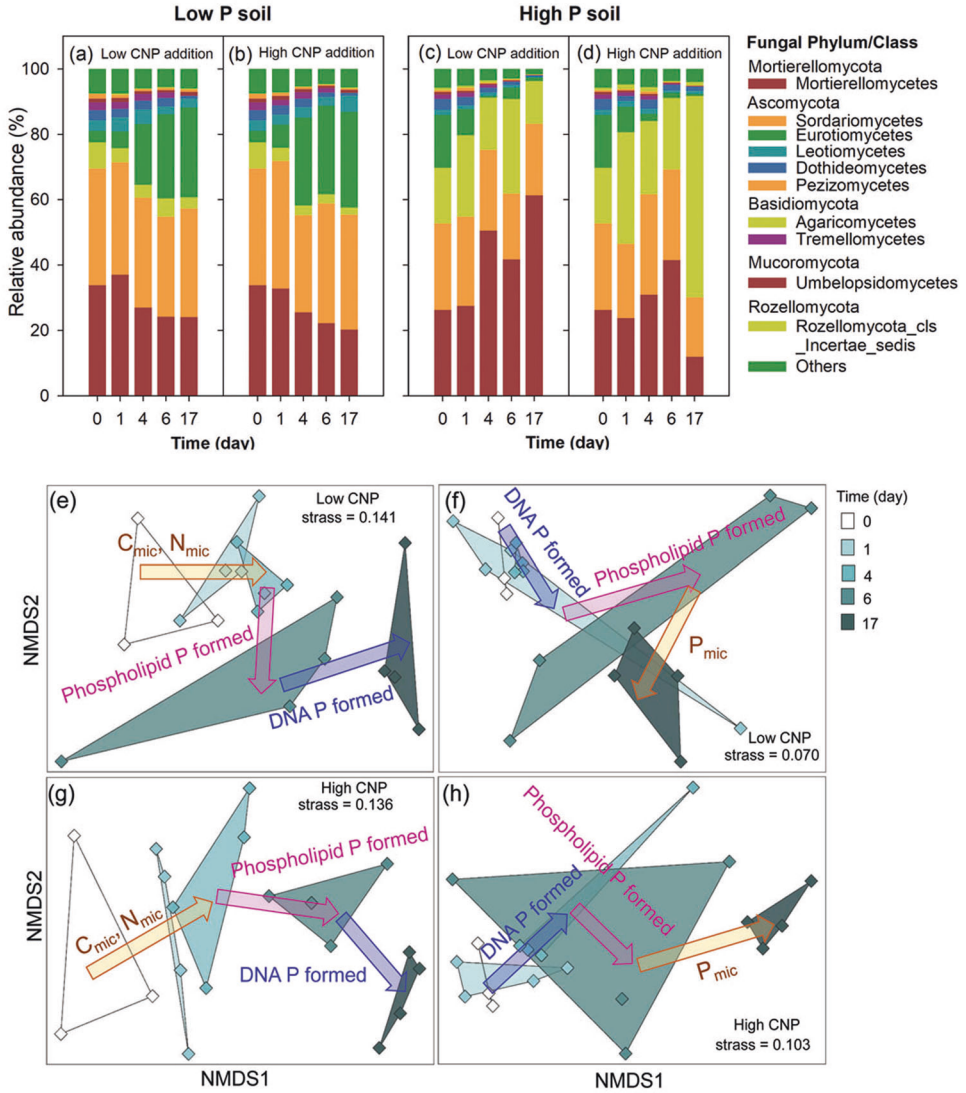

Fig. 4 Overview of changes in relative abundance of the dominant fungal taxa and related processes following sequential P and CN additions at two contrasting levels in the low P and high P soils. Changes in fungal community composition are indicated by shifts in relative abundance of the top 10 bacterial classes affiliating to 5 phyla (**a**–**d**). Simplified non-metric multidimensional scaling (NMDS) plots derived from sequence data at OTU level (**e**–**h**). There are three replicates in the day 0, and four replicates in other sampling days. Areas marked by different colors in NMDS plots separate the community composition before and after CNP additions, and arrows show most important processes of microbial biomass, phospholipids P and DNA P formation (canonical correspondence analysis, $p < 0.05$).

DISCUSSION

Microbial P incorporation into DNA and phospholipids is controlled by soil P and C availability

This study aimed to understand whether our classical view on de-novo synthesis versus recycling of major P compounds (DNA and phospholipids) could be valid irrespective of the stoichiometric conditions or whether, alternatively, microorganisms deviated from stoichiometric homeostasis by modifying their intra- and extracellular P utilization strategies to adapt to nutrient deficiency.

We observed a greater re-allocation of immobilized P to DNA and hence formation of de-novo DNA P but without microbial growth (i.e. a marked increase in DNA content) before C N addition in both the low and high P soils (Figs. 1, 2). Microorganisms might expend the provided P to repair genomic DNA to avoid mutations, e.g. by DNA methyltransferases [50], when sufficient P was available but growth was C limited. This element allocation pattern is termed mode 2 in Fig. 7. In contrast, less P was incorporated into phospholipids irrespective of soil P availability before microbial growth, which partly disagreed with our first hypothesis of a higher P incorporation into phospholipids than into DNA in the low P soil. Such a discrepancy can potentially be ascribed to limitation of available C, supporting the synthesis of C backbones required for phospholipids formation [51]. Under C starvation, microbial cell-size decreases because cells partially "digest" themselves and only leave essential cell compartments remaining [52]. This strategy is channeled into maintaining functions and turnover of essential cell materials containing major nutrients (including C and P) in the effort to survive [53]. Thus, DNA repair was still supported, but no longer the de-novo formation of phospholipids because they could be substitute by lipids without P (i.e., betaine lipids) [34]. Thus, the C required in this phase (i.e. for DNA backbone repair) was covered by compounds in the cytosol, as indicated by a decrease in C_{mic} (determined solely in water-extractable microbial compounds). Other nutrients, especially P in microorganisms (P_{mic}), in turn, increased to ensure that all deficiencies except C were removed ([54], Table S2). Besides, the P_{mic} increase might also be ascribed to the preparation of RNA during DNA repairation [50, 55].

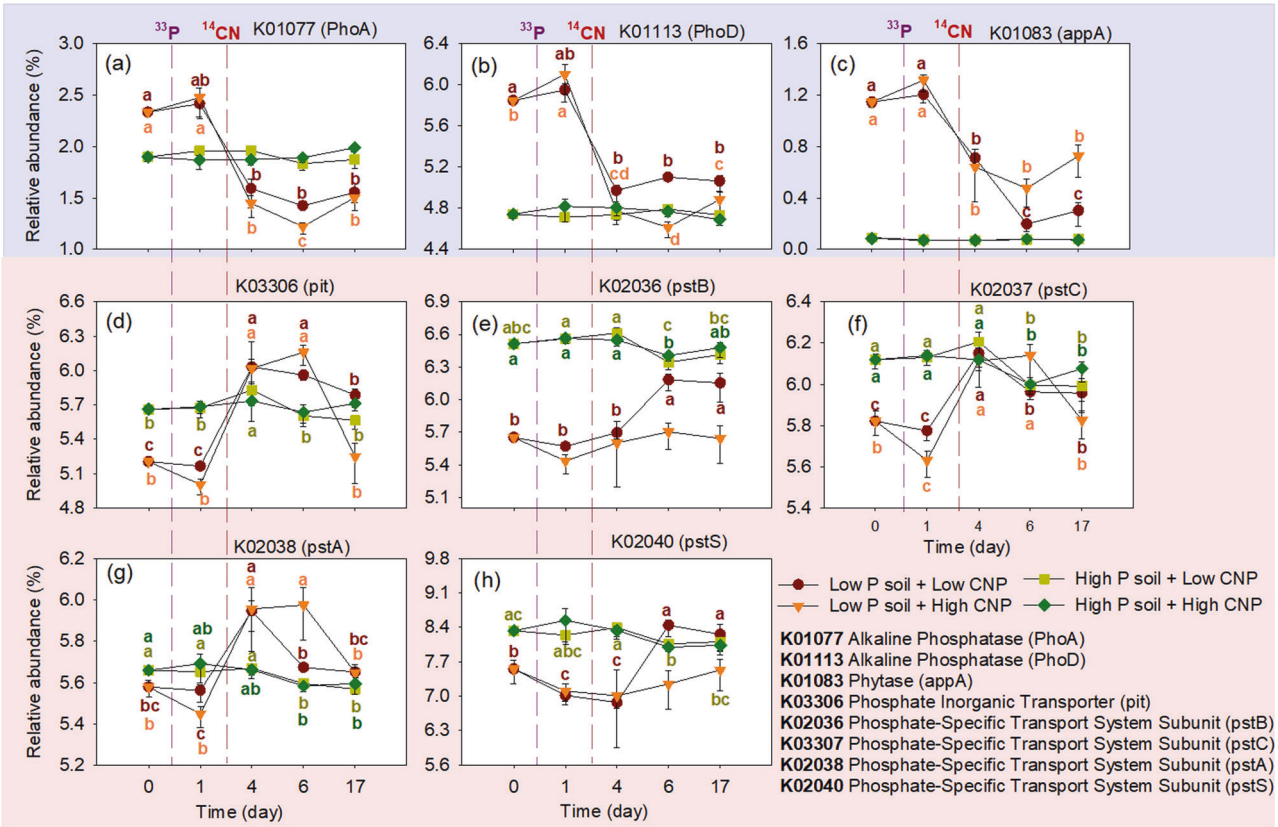

Fig. 5 Dynamics in relative abundances of functional genes involved in microbial P cycling. The genes coding selected enzymes responsible for organic P mineralization (**a**–**c**) and uptake and transformation (**d**–**h**) depending on CNP additions are displayed. Blue arrows and dash lines indicate P addition, and pink arrows and dash lines note CN addition. Symbols indicate the genes with annotations taken from the Kyoto Encyclopedia of Genes and Genomes (KEGG) [73]. Lowercase letters indicate significant difference among sampling dates within one treatment with $p < 0.05$, and the treatment is indicated by the color of the letters.

The addition of high level C N substantially increased de-novo DNA and phospholipids P synthesis as well as phosphate P incorporation. This was paralleled by a marked increase in DNA and C_{mic} (Table S2, Figs. 1, 2), indicating a replicative microbial growth. Moreover, we observed a strong C incorporation into DNA and phospholipids along with this microbial growth (Fig. S10, S11). These findings revealed a strong C limitation for growth and for microbial P incorporation in both the high and low P soils [35]. Our second hypothesis that both the phospholipids and DNA P incorporation will be intensified by increased C availability could thus be confirmed. The relative incorporation rate of P into DNA and phospholipids, however, differed between the low and high P soils, reflecting a contrasting cellular P management prior to growth. In the low P soil, greater ^{33}P proportion was re-allocated to the phospholipids (24%) from total ^{33}P incorporated into biomass as compared with the portion re-allocated to DNA (15%) following CN addition. This partly confirmed our first hypothesis of a higher P incorporation into phospholipids than into DNA in low P soils when C deficiency is removed. Moreover, the new phospholipids P was formed prior to DNA P formation, and more P was allocated to the phospholipids than to DNA (Fig. 2). Especially under low level CN amendments in the low P soil, the phospholipids P increased immediately while the increase of DNA P lagged two days behind. This decoupling between phospholipids P formation and DNA production suggests a preferential P allocation to membrane lipids before microbial growth, which matches a recently described phenomenon that phospholipids may serve as a microbial P storage to be exhausted under strong P deficiency but to be refilled internally when functionally diverse membranes are needed during growth [56]. For example, by comparing the composition of dominant polar lipids among sites with various soil P status, Warren [34] demonstrated a decrease in phospholipids while an increase in betaine lipids – P-free analog as soil P availability declined, and suggested substitution of phospholipids with betaine lipids as one potential mechanism for microbial adaptation to P deficiency [34]. Such use of membranes to store P enables P turnover from phospholipids within cells without release into the soil, leading to a more conservative and energy-saving P recycling displayed as mode 1 in Fig. 7. Our metagenome data reflected that the genetic traits enabling this high plasticity in membrane P contents was specifically represented in distinct microbial community members. Thus, community shifts, driven by increased C availability, may go along with increase in this trait (see discussion below). Besides P storage, removal of P deficiency was also evident in the cytosol by a concomitant increase in P_{mic} forming the basic P pool to guarantee the DNA reparation and later the de-novo formation of phospholipids P. Given that the P_{mic} extraction captures some polyphosphates (polyP), the most likely phenomenon we observed here is also the "refill" of the polyP pools within microbial cells. Generally, mode 3 in Fig. 7 characterizes the refill of depleted P pools with a potential priority DNA > polyP > phospholipids, which need to be further confirmed in follow-up studies. Moreover, the increase of P_{mic} and C_{mic} during P refill shifted the microbial stoichiometry towards a value approaching that of the high P soil, where the microorganisms were ready to grow (Table S2). This suggests the complete overcome of nutrient limitation (but also no C excess) after P and C addition. It also suggests that the P content of membrane lipids is key to microbial strategies balancing their cellular element stoichiometry.

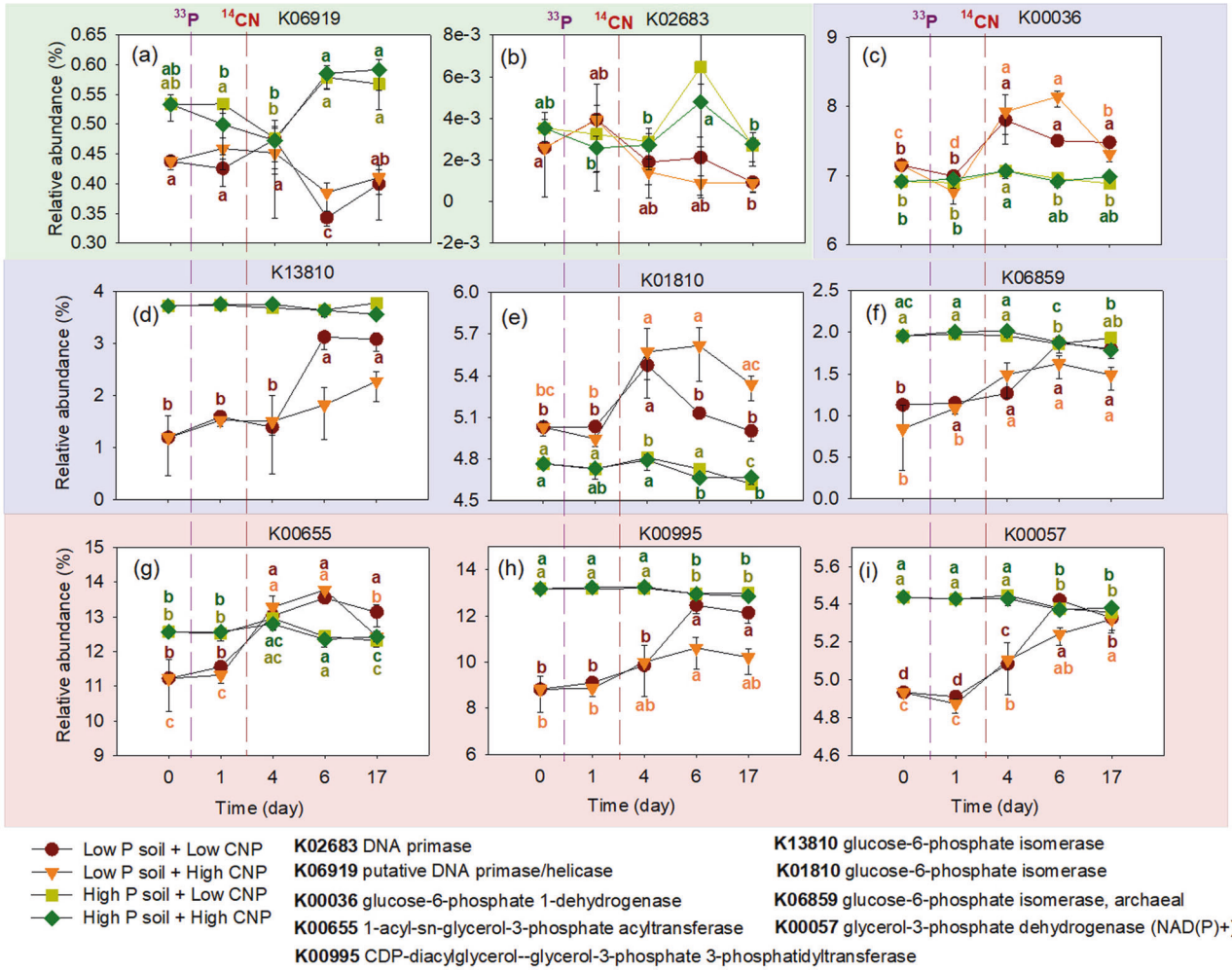

Fig. 6 Dynamics in relative abundances of functional genes involved in microbial intracellular metabolisms. The genes coding selected enzymes responsible for DNA synthesis (**a**, **b**) and metabolisms of phospholipids compounds (**c**–**i**) are displayed. Blue arrows and dash lines indicate P addition and pink arrows and dash lines note CN addition. Symbols indicate the genes with annotations taken from the Kyoto Encyclopedia of Genes and Genomes (KEGG) [51]. Lowercase letters indicate significant difference among sampling dates within one treatment with $p < 0.05$, and the treatment is indicated by the color of the letters.

In high P soil, the increment of de-novo phospholipids and DNA P caused by CN addition was synchronous with a marked increase in DNA content (Table S2, Fig. 1b, d). Importantly, the microorganisms re-allocated a disproportionately high P proportion to DNA (1.1%) than to phospholipids (0.4%) during the entire incubation period (Fig. 2b, d). This could confirm that DNA synthesis consumes a high proportion of the P uptake when cells are in a replicative growth mode, not only due to the biosynthetic demand for DNA and surely also high RNA demands itself but also due to fact that cells do not focus on other processes of nutrient storage in this period [25]. Here by tracing the intracellular pathway of P allocation with ^{33}P labeling, we experimentally verified for the first time the putatively considerable P incorporation into DNA by rapidly replicating microorganisms. Given that the nucleic acids contain 40-70% of the total microbial P [3], the release of newly formed nucleic acids after microbial death following exponential growth will result in an "open" soil P cycling described as mode 4 in Fig. 7.

In general, our results confirm that C deficiency exceeds P limitation for microorganisms irrespective of the original soil P availability. When increased C availability is sufficient to induce microbial growth in low P soil (i.e., high CNP addition to low P soil), the limited elements (C and P) will be incorporated into the cytosol, and all P pools including that of the membrane lipids need to be refilled before replicative microbial growth can start. This observation confirms that especially membrane phospholipids can serve as microbial P storage to be used internally upon P exhaustion, but need to be refilled before replication. In contrast, soil available P will instantaneously be incorporated into DNA for replication in high P soil if C is available in adequate quantities for microbial growth (i.e., high CNP addition to high P soil). This will accelerate extracellular P turnover between cells through replicative growth and subsequent growth-death dynamics, i.e. P allocation between necromass and living cells [57]. Thus, the P recycling within microbial cells is more conservative in originally P-limited soil by restoring and exhausting phospholipids P intracellularly, inducing the highly dynamic phospholipids P pool. Accordingly, previous studies using DNA P turnover to represent microbial biomass P turnover have missed the significantly higher dynamics of phospholipids [48]. Those dynamics, however, play an important role in soil P cycling, especially under P limitation. We therefore recommend considering both DNA and phospholipids in experiments aiming to understand the microbiome's control over soil P turnover. However, further studies are necessary to characterize the microbial component-specific P turnover under a broader context of nutrient conditions and to test the generality of these findings across soil types.

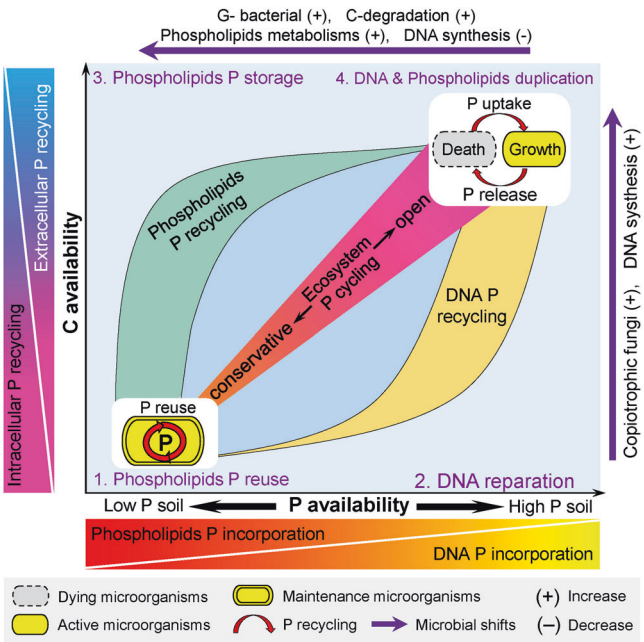

Fig. 7 Conceptual figure illustrating the relative P incorporation rate into microbial phospholipids and DNA pools and the dominance of extra- and inter-cellular P recycling in soils with contrasting P availability (X-axis), and their response to changes in soil C availability (Y-axis). Four modes and the specific mechanistic features underlie them have been proposed: 1. Low C availability in low P soil: rapid P recycling in microbial phospholipids is common because intensive P incorporation into phospholipids and rapid intracellular P recycling. The P from phospholipids is intensively reused within the cells through endogenous metabolism to support microbial maintenance without P release into soil solution, resulting in a more "conservative" ecosystem P cycling. 2. Low C availability in high P soil: soil microorganisms preferentially incorporate P into DNA for DNA reparation but without cell division. This facilitates the shifts of microorganisms from maintenance to the state of ready to grow, because preparation of the accurate and intact genetic information can help with the immediate start of microbial growth. 3. High C availability in low P soil, a disproportionately large P amount is incorporated into phospholipids mainly due to P "refill" of the depleted phospholipids pool. Phospholipids serves as an efficient P storage to resist to further P exhaustion following microbial growth. 4. High C availability in high P soil: P is invested for DNA and phospholipids duplication, but a disproportionately large amount of immobilized P is re-allocated to DNA to meet the boost of nucleic acids demand during rapid growth, leading to a faster DNA recycling. In this case, the extracellular P recycling is accelerated via taking up the P released from dying microorganisms by growing ones, which consequently results in an "open" P cycling in soil. Generally, a DNA P incorporation pattern coupled with intensified extracellular P recycling dominates in soils with high nutrient and high C availability, whereas a phospholipids P incorporation pattern with intensified intracellular P recycling dominates the soils depleted in nutrients and C. The concomitant shifts of fungal composition towards copiotrophs and microbial functions towards DNA synthesis after removal of C deficiency drive transformations from pattern 2 to pattern 4. However, bacterial compositional shifts towards G- and functional switch with strong organic C degradation and phospholipids metabolisms after P exhaustion can induce transformations from pattern 4 to pattern 3.

Implications of soil bacterial structure and functions on cellular P dynamics

Various soil microorganisms are characterized by specific cell structures [58], life strategies [59, 60], and functions in C and nutrient acquisition [61]. These characteristics enable microorganisms to respond differently to changes in soil P availability and hence feedback to distinct P utilization strategies. In this study, we found a strong shift in bacterial composition in the low P soil accompanied by an increase in phospholipids rather DNA P following P amendment (Fig. 3e, g, S6a). One explanation is linked to the substantial increment in G- bacteria (Proteobacteria), as they have an additional phospholipids bilayer in the outer cell membrane, making their phospholipids P content twice that of G + bacteria [20, 30]. This, however, disagrees with our hypothesis that a boost of G- bacteria in low P soil requires the removal of C starvation. This unexpected increase in G- abundance prior to C addition can be explained by the specific groups growing, namely G- bacteria with a strong hydrolytic ability, such as Burkholderia [62] (Fig. S2). Concomitant increases in the abundance of C-degrading genes further confirmed this function of these G- bacteria in soils (Fig. S7a, c). Such a switch in the microbial composition towards an increased functional potential for C acquisition might be a community strategy to resist the co-limitation of C and P. The increased Burkholderia abundance, however, was counteracted by an enrichment of oligotrophic groups two days later, such as Acidobacteria, Verrucomicrobia, and Chloroflexi [63] as result of the exhaustion of the available C pool. Given that P could be reused intracellularly through phospholipids turnover and by substituting the phospholipids with lipids containing no P (i.e., betaine lipids), the C deficiency might rapidly become dominant again after exhaustion in soil solution. The P, however, could be reused intracellularly through rapid phospholipids turnover, as we found an enrichment in genes responsible for the biosynthesis or hydrolysis of key phospholipids components (Fig. 6c–i). These observations confirm our expectation of a high plasticity of the phospholipids metabolisms, explaining our dynamic, and growth-independent phospholipids P incorporation pattern [64].

Differing from those in the low P soil, the community composition of bacteria in high P soil was relatively stable while the genes coding putative DNA primase increased substantially following CNP addition (Fig. 6a, b), suggesting an initial growth of copiotrophic bacteria. Perhaps, the rapid multiplication of copiotrophic bacteria can increase soil C and nutrient accessibility for their oligotrophic counterparts by producing large amounts of necromass through intensive growth-death dynamics [16, 57]. The concomitant dynamics of copiotrophs and oligotrophs can help retain an overall stable community composition over the course of the incubation irrespective of changing resource stoichiometry. This was further supported by the significant associations between bacterial composition and de-novo formed DNA P content in high P soil (Fig. S3b, d). All these confirmed an intensive microbial growth-death dynamic under the DNA P incorporation pattern, and supported our suggestion of an extracellular P cycling in P-rich soils.

Implications of soil fungal structure and functions on cellular P dynamics

Compared to bacteria, soil fungi responded less to P addition in low P soil, but their composition shifted markedly following CN application (Figs. S2, S4). This disagreed with previous field studies demonstrating greater effects of P fertilization on fungal versus bacterial communities [65]. Adding CN to low P soil enriched the fungal groups specialized in degrading recalcitrant organics, e.g., Eurotiomycetes, which include the typical soft rot [66], suggesting that the amount of applied CNP (200% C_{mic}, N_{mic} and P_{mic} of the original soil) can stimulate the microbial potentials in C mineralization. This phenomenon can be interpreted by the "microbial stoichiometric decomposition" hypothesis, that is, soil C mineralization will be stimulated by increased microbial activity when nutrients sufficiently meet microbial stoichiometric requirements [67]. Such a shift in fungal communities related to C mineralization could also increase the C accessibility to bacteria and boost the G- bacteria abundance, the formation of their outer membranes and thus the increase in P incorporation into phospholipids. This

linkage is confirmed by our SEM showing strong indirect effects of fungal composition on phospholipids P content (by influencing bacterial composition) (Fig. S6a).

In high P soil, CNP addition induced a clear shift towards copiotrophic fungi (rapid growth rate), i.e., Agaricomycetes and Mortierellomycetes [68, 69], which might further cause an increase in DNA P incorporation [25] (Fig. 4f, h, S6b). Additionally, we found that bacteria exerted an indirect effect on DNA P incorporation by affecting fungal community composition (Fig. 3f, h, S6b). One possible reason is that some fungal communities, i.e., those affiliating to Mortierellomycetes, can foster endobacteria and take advantage of their bacterial partner to improve their nutrition [70–72].

Overall, the phospholipids P incorporation in low P soil was strongly related to an enrichment of G- bacteria and an increased potential in phospholipids metabolisms. The preferential allocation of P to DNA in high P soil, however, was largely related to fungal shifts towards copiotrophs and a bacterial functional switch to high DNA synthesis potentials (as a prerequisite for the observed rapid replicative growth). These findings confirmed our third hypothesis that the contrasting P incorporation into cells driven by C availability are in feedback with shifts in microbiome composition and functions.

CONCLUSIONS

By combining ^{33}P and ^{14}C labeling with tracing of bacterial and fungal community biomarkers and functional genes, we disengaged the role of DNA and phospholipids in soil P cycling. Four modes of P allocation within and among microbial cells were unrevealed and linked to key microbial taxa and indicative functional genes. By that we advanced our insights into the mechanisms of microbial intra- and extracellular P recycling facing stoichiometry imbalance. Generally, adaptation to overall low P availability accelerates microbial intracellular P recycling and reduce microbial P release from cells. Whenever rapid use or refill of the phospholipids pool is required, this is linked to high abundances of microbial community members (e.g. some G-) with a fast phospholipids turnover. In contrast, a rapid extracellular P recycling may dominate the community of the high P soils based on a large release of nucleic acids and surely all other cell P pools during intensive microbial growth and death dynamics. This is associated with a strong enrichment of fungal copiotrophs and microbial genes coding DNA primase. We predict that an ongoing relative P depletion in soils can cause a shift in microbial functioning from the dominance of P cycling through extracellular release of microbial DNA by growth-death dynamics towards a dominance of P recycle through intracellular phospholipids P reuse.

DATA AVAILABILITY

Raw DNA sequence files were deposited in the GenBank via BioProject accession PRJNA860331. Other data that support the findings of this study are available from the corresponding author upon reasonable request.

REFERENCES

1. Peñuelas J, Sardans J. The global nitrogen-phosphorus imbalance. Science. 2022;375:266–7.
2. Panikov NS. Microbial growth kinetics. London: Chapman Hall; 1995.
3. Bünemann EK, Prusisz B, Ehlers K. Characterization of phosphorus forms in soil microorganisms, In: Bünemann EK et al. eds. Phosphorus in action, soil biology. Verlag GmbH, Heidelberg: Springer; 2011; 26. p. 37–58.
4. Sohrt J, Lang F, Weiler M. Quantifying components of the phosphorus cycle in temperate forests. Wiley Interdiscip Rev Water. 2017;4:e1243.
5. Scheerer U, Trube N, Netzer F, Rennenberg H, Herschbach C. ATP as phosphorus and nitrogen source for nutrient uptake by *Fagus sylvatica* and *Populus x canescens* roots. Front Plant Sci. 2019;10:378.
6. Frossard E, Condron LM, Oberson A, Sinaj S, Fardeau JC. Processes governing phosphorus availability in temperate soils. J Environ Qual. 2000;29:15.
7. Kruse J, Abraham M, Amelung W, Baum C, Bol R, Kühn O, et al. Innovative methods in soil phosphorus research: a review. J Plant Nutr Soil Sci. 2015;178:43–88.
8. Maranguit D, Guillaume T, Kuzyakov Y. Land-use change affects phosphorus fractions in highly weathered tropical soils. Catena. 2017;149:385–93.
9. Stutter MI, Shand CA, George TS, Blackwell MSA, Bol R, MacKay RL, et al. Recovering phosphorus from soil: a root solution? Environ Sci Technol. 2012;46:1977–8.
10. Baldrian P. Forest microbiome: diversity, complexity and dynamics. FEMS Microbiol Rev. 2017;41:109–30.
11. Koukol O, Novak F, Hrabal R, Vosatka M. Saprotrophic fungi transform organic phosphorus from spruce needle litter. Soil Biol Biochem. 2006;38:3372–9.
12. Wright SJ, Guo X, Tringe SG, Tfaily MM, Paša-Tolić L, Hazen TC, et al. Community proteogenomics reveals the systemic impact of phosphorus availability on microbial functions in tropical soil. Nat Ecol Evol. 2018;2:499–509.
13. Yuan XB, Niu DC, Gherardi LA, Liu YB, Wang Y, Elser JJ, et al. Linkages of stoichiometric imbalances to soil microbial respiration with increasing nitrogen addition: evidence from a long-term grassland experiment. Soil Biol Biochem. 2019;138:107580.
14. Oberson A, Joner EJ. Microbial turnover of phosphorus in soil, In: BL Turner BL et al. eds. Organic phosphorus in the environment. Oxfordshire, UK: CABI Publishing; 2005.
15. Chen J, Seven J, Zilla T, Dippold MA, Blagodatskaya E, Kuzyakov Y. Microbial C:N:P stoichiometry and turnover depend on nutrients availability in soil: A ^{14}C, ^{15}N and ^{33}P triple labelling study. Soil Biol Biochem. 2019;131:206–16.
16. Miltner A, Bombach P, Schmidt-Brücken B, Kästner M. SOM genesis: microbial biomass as a significant source. Biogeochemistry. 2012;111:41–55.
17. Kouno K, Wu J, Brookes PC. Turnover of biomass C and P in soil following incorporation of glucose or ryegrass. Soil Biol Biochem. 2002;34:617–22.
18. Lang F, Bauhus J, Frossard E, George E, Kaiser K, Kaupenjohann M, et al. Phosphorus in forest ecosystems: new insights from an ecosystem nutrition perspective. J Plant Nutr Soil Sci. 2016;179:129–35.
19. Mine AH, Coleman ML, Colman AS. Phosphorus release and regeneration following laboratory lysis of bacterial cells. Front Microbiol. 2021;12:641700.
20. Blagodatskaya E, Kuzyakov Y. Active microorganisms in soil: critical review of estimation criteria and approaches. Soil Biol Biochem. 2013;67:192–211.
21. Dippold MA, Kuzyakov Y. Direct incorporation of fatty acids into microbial phospholipids in soils: position-specific labeling tells the story. Geochimica Et Cosmochimica Acta. 2016;174:211–21.
22. De Nobili M, Contin M, Mondini C, Brooks PC. Soil microbial biomass is triggered into activity by trace amounts of substrate. Soil Biol Biochem. 2001;33:1163–70.
23. Blagodatskaya E, Blagodatsky S, Anderson TH, Kuzyakov Y. Microbial growth and carbon use efficiency in the rhizosphere and root-free soil. PLoS ONE. 2014;9:e93282.
24. Webley DM, Jones, D. Biological transformations of microbial residues in soil, In: AD McLaren et al. Eds. Soil biochemistry. New York, USA: Marcel Dekker; 1971.
25. Elser JJ, Sterner RW, Gorokhova E, Fagan WF, Markow TA, Cotner JB, et al. Biological stoichiometry from genes to ecosystems. Ecol Lett. 2000;3:540–50.
26. Reyes-Lamothe R, Sherratt DJ. The bacterial cell cycle, chromosome inheritance and cell growth. Nat Rev Microbiol. 2019;17:467–78.
27. Makino W, Cotner JB, Sterner RW, Elser JJ. Are bacteria more like plants or animals? Growth rate and resource dependence of bacterial C:N:P stoichiometry. Funct Ecol. 2003;17:121–30.
28. Zengler K. Central role of the cell in microbial ecology. Microbiol Mol Biol Rev. 2009;73:712–29.
29. Mouginot C, Kawamura R, Matulich KL, Berlemont R, Allison SD, Amend AS, et al. Elemental stoichiometry of fungi and bacteria strains from grassland leaf litter. Soil Biol Biochem. 2014;76:278–85.
30. Chatterjee SN, Chaudhuri K. Gram-negative bacteria: the cell membranes. In: Outer membrane vesicles of bacteria. Springer briefs in microbiology. Berlin, Heidelberg: Springer; 2012.
31. Elser JJ, Dobberfuhl DR, MacKay NA, Schampel JH. Organism Size, Life History, and N:P Stoichiometry: toward a unified view of cellular and ecosystem processes. BioScience. 1996;46:674–84.
32. Rousk J, Brookes P, Bååth E. The microbial PLFA composition as affected by pH in an arable soil. Soil Biol Biochem. 2010;42:516–20.
33. Bore EK, Halicki S, Kuzyakov Y, Dippold MA. Structural and physiological adaptations of soil microorganisms to freezing revealed by position-specific labeling and compound-specific ^{13}C analysis. Biogeochemistry. 2019;143:207–19.
34. Warren CR. Soil microbial populations substitute phospholipids with betaine lipids in response to low P availability. Soil Biol Biochem. 2020;140:107655.

35. Soong JL, Fuchslueger L, Maranon-Jimenez S, Torn MS, Janssens IA, Penuelas J, et al. Microbial carbon limitation: the need for integrating microorganisms into our understanding of ecosystem carbon cycling. Global Change Biol. 2019;26:1953–61.
36. Joergensen RG, Wu JS, Brookes PC. Measuring soil microbial biomass using an automated procedure. Soil Biol Biochem. 2011;43:873–6.
37. Brookes PC, Landman A, Pruden G, Jenkinson DS. Chloroform fumigation and the release of soil nitrogen: a rapid direct extraction method to measure microbial biomass nitrogen in soil. Soil Biol Biochem. 1985;17:837–42.
38. Cheesman AW, Turner BL, Reddy KR. Interaction of phosphorus compounds with anion-exchange membranes: implications for soil analysis. Soil Sci Soc Am J. 2010;74:1607.
39. Kouno K, Tuchiya Y, Ando T. Measurement of soil microbial biomass phosphorus by an anion exchange membrane method. Soil Biol Biochem. 1995;27:1353–7.
40. d'Angelo E, Crutchfield J, Vandiviere M. Rapid, sensitive, microscale determination of phosphate in water and soil. J Environ Qual. 2001;30:2206–9.
41. Bilyera N, Blagodatskaya E, Yevdokimov I, Kuzyakov Y. Towards a conversion factor for soil microbial phosphorus. Eur J Soil Biol. 2018;87:1–8.
42. Caporaso JG, Lauber CL, Walters WA, Berg-Lyons D, Huntley J, Fierer N, et al. Ultra-high-throughput microbial community analysis on the Illumina HiSeq and MiSeq platforms. ISME J. 2012;6:1621–4.
43. Bellemain E, Carlsen T, Brochmann C, Coissac E, Taberlet P, Kauserud H. ITS as an environmental DNA barcode for fungi: an *in silico* approach reveals potential PCR biases. BMC Microbiol. 2010;10:189.
44. Abarenkov K, Nilsson RH, Larsson KH, Alexander IJ, Eberhardt U, Erland S, et al. The UNITE database for molecular identification of fungi-recent updates and future perspectives. New Phytol. 2010;186:281.
45. Jun S-R, Robeson MS, Hauser LJ, Schadt CW, Gorin AA. PanFP: pangenome-based functional profiles for microbial communities. BMC Res Notes. 2015;8:479.
46. Frostegård Å, Tunlid A, Bååth E. Microbial biomass measured as total lipid phosphate in soils of different organic content. J Microbiol Methods. 1991;14:151–63.
47. Gunina A, Dippold MA, Glaser B, Kuzyakov Y. Fate of low molecular weight organic substances in an arable soil: from microbial uptake to utilisation and stabilisation. Soil Biol Biochem. 2014;77:304–13.
48. Spohn M, Widdig M. Turnover of carbon and phosphorus in the microbial biomass depending on phosphorus availability. Soil Biol Biochem. 2017;113:53–59.
49. Bünemann EK. Assessment of gross and net mineralization rates of soil organic phosphoruse a review. Soil Biol Biochem. 2015;89:82–98.
50. Samson L. The suicidal DNA repair methyltransferases of microbes. Mol Microbiol. 1992;6:825–31.
51. Park Y, Solhtalab M, Thongsomboon W, Aristilde L. Strategies of organic phosphorus recycling by soil bacteria: acquisition, metabolism, and regulation. Environ Microbiol Rep. 2022;14:3–24.
52. Murphy DJ. The dynamic roles of intracellular lipid droplets: from archaea to mammals. Protoplasma. 2012;249:541–85.
53. Mason CA, Hamer G, Bryers JD. The death and lysis of microorganisms in environmental processes. FEMS Microbiol Lett. 1986;39:373–401.
54. Bünemann EK, Oberson A, Liebisch F, Keller F, Annaheim KE, Huguenin-Elie O, et al. Rapid microbial phosphorus immobilization dominates gross phosphorus fluxes in a grassland soil with low inorganic phosphorus availability. Soil Biol Biochem. 2012;51:84–95.
55. Blagodatsky SA, Heinemeyer O, Richter J. Estimating the active and total soil microbial biomass by kinetic respiration analysis. Biol Fertil Soils. 2000;32:73–81.
56. Heuck C, Weig A, Spohn M. Soil microbial biomass C: N: P stoichiometry and microbial use of organic phosphorus. Soil Biol Biochem. 2015;85:119–29.
57. Cui J, Zhu Z, Xu X, Liu S, Jones DL, Kuzyakov Y, et al. Carbon and nitrogen recycling from microbial necromass to cope with C:N stoichiometric imbalance by priming. Soil Biol Biochem. 2020;142:107720.
58. Brown L, Wolf J, Prados-Rosales R, Casadevall A. Through the wall: extracellular vesicles in Gram-positive bacteria, mycobacteria and fungi. Nat Rev Microbiol. 2015;13:620–30.
59. Leff JW, Jones SE, Prober SM, Barberána A, Borere ET, Firn JL, et al. Consistent responses of soil microbial communities to elevated nutrient inputs in grasslands across the globe. PNAS. 2015;112:10967–72.
60. Malik AA, Martiny JBH, Brodie EL, Martiny AC, Treseder KK, Allison SD. Defining trait-based microbial strategies with consequences for soil carbon cycling under climate change. ISME J. 2020;14:1–9.
61. Cardenas E, Kranabetter JM, Hope G, Maas KR, Hallam S, Mohn WW. Forest harvesting reduces the soil metagenomic potential for biomass decomposition. ISME J. 2015;9:2465–76.
62. Rosenberg E, DeLong EF, Lory S, Stackebrandt E, Thompson F, (Eds.) 2014. The prokaryotes: alphaproteobacteria and betaproteobacteria. 4th ed. Heidelberg: Springer; 2012.
63. Ho A, Di Lonardo DP, Bodelier PL. Revisiting life strategy concepts in environmental microbial ecology. FEMS Microbiol Ecol. 2017;93:fix006.
64. Konstantinidis KT, Tiedje JM. Trends between gene content and genome size in prokaryotic species with larger genomes. PNAS. 2004;101:3160–5.
65. Widdig M, Heintz-Buschart A, Schleuss P-M, Guhr A, Borer ET, Seabloom EW, et al. Effects of nitrogen and phosphorus addition on microbial community composition and element cycling in a grassland soil. Soil Biol Biochem. 2020;151:108041.
66. Lundell TK, Mäkelä MR, de Vries RP, Hildén KS. Genomics, lifestyles and future prospects of wood-decay and litter-decomposing basidiomycota. Adv Bot Res. 2014;70:329–70.
67. Zhu ZK, Fang YY, Liang YQ, Li YH, Liu SL, Li YF, et al. Stoichiometric regulation of priming effects and soil carbon balance by microbial life strategies. Soil Biol Biochem. 2022;169:108669.
68. Kersten P, Cullen D. Recent advances on the genomics of litter- and soil-inhabiting agaricomycetes. In: Horwitz B, Mukherjee P, Mukherjee M, Kubicek C, eds. Genomics of soil- and plant-associated fungi. Soil biology, vol 36. Berlin, Heidelberg: Springer; 2013.
69. Tedersoo L, Bahram M, Põlme S, Kõljalg U, Yorou NS, Wijesundera R, et al. Global diversity and geography of soil fungi. Science. 2014;346:1256688.
70. Uehling J, Gryganskyi A, Hameed K, Tschaplinski T, Misztal PK, Wu S, et al. Comparative genomics of *Mortierella elongata* and its bacterial endosymbiont Mycoavidus cysteinexigens. Environ Microbiol. 2017;19:2964–83.
71. Partida-Martínez LP. The fungal holobiont: evidence from early diverging fungi. Environ Microbiol. 2017;19:2919–23.
72. Desirò A, Hao Z, Liber JA, Benucci GMN, Lowry D, Roberson R. Mycoplasma-related endobacteria within Mortierellomycotina fungi: diversity, distribution and functional insights into their lifestyle. ISME J. 2018;12:1743–57.
73. Bergkemper F, Scholer A, Engel M, Lang F, Kruger J. Phosphorus depletion in forest soils shapes bacterial communities towards phosphorus recycling systems. Environ Microbiol. 2016;18:2767.

ACKNOWLEDGEMENTS

We thank Evgenia Blagodatskaya, Huadong Zang, Callum Banfield, Deejay Maranguit, and Karin Schmidt for their help during the incubation experiment. We also thank the Center for Stable Isotopes (KOSI) in Göttingen for fast and reliable measurement of stable isotope samples, and the Radioisotope Laboratory (LARI) for their support in handling the radioisotope tracers.

AUTHOR CONTRIBUTIONS

Conceptualization was developed by JC, MAD, and YK Experiment was done by JC, JS, and TZ Data analyses were done by JC. and HX. All the authors interpreted and wrote the manuscript.

FUNDING

We sincerely thank the Central Public-interest Scientific Institution Basal Research Fund, China (CAFYBB2020QB003), and the China Scholarship Council (CSC), National Natural Science Foundation of China (31901161) for funding Jie Chen. This work was done in the framework of the DFG special priority program 1685 "Ecosystem nutrition: Forest strategies for limited phosphorus resources" within the project DFG KU 1184/36-1, and the RUDN University Strategic Academic Leadership Program. We greatly acknowledge funding by the German Research Foundation (DFG) also within DI 2136/6 within the priority program 1685 and the Robert-Bosch Foundation for funding M. Dippold in the framework of the Junior-Professorship 2017.

COMPETING INTERESTS

The authors declare no competing interests.

ADDITIONAL INFORMATION

Supplementary information The online version contains supplementary material available at https://doi.org/10.1038/s43705-023-00340-7.

Correspondence and requests for materials should be addressed to Jie Chen.

Reprints and permission information is available at http://www.nature.com/reprints

Publisher's note Springer Nature remains neutral with regard to jurisdictional claims in published maps and institutional affiliations.